



# Jet injection studies for partially baffled mixing reactors: a general correlation for the jet trajectory and jet penetration depth

Jean-Philippe Torré, David F. Fletcher, Iréa Touche, Thierry Lasuye, Catherine Xuereb

## ► To cite this version:

Jean-Philippe Torré, David F. Fletcher, Iréa Touche, Thierry Lasuye, Catherine Xuereb. Jet injection studies for partially baffled mixing reactors: a general correlation for the jet trajectory and jet penetration depth. Chemical Engineering Research and Design, 2008, 86 (10), pp.1117-1127. 10.1016/j.cherd.2008.05.005 . hal-03577232

**HAL Id: hal-03577232**

**<https://hal.science/hal-03577232>**

Submitted on 16 Feb 2022

**HAL** is a multi-disciplinary open access archive for the deposit and dissemination of scientific research documents, whether they are published or not. The documents may come from teaching and research institutions in France or abroad, or from public or private research centers.

L'archive ouverte pluridisciplinaire **HAL**, est destinée au dépôt et à la diffusion de documents scientifiques de niveau recherche, publiés ou non, émanant des établissements d'enseignement et de recherche français ou étrangers, des laboratoires publics ou privés.



## Open Archive Toulouse Archive Ouverte (OATAO)

OATAO is an open access repository that collects the work of Toulouse researchers and makes it freely available over the web where possible.

This is an author-deposited version published in: <http://oatao.univ-toulouse.fr/>  
Eprints ID : 3017

**To link to this article :**

URL : <http://dx.doi.org/10.1016/j.cherd.2008.05.005>

To cite this version: Torr , Jean-Philippe and Fletcher, David F. and Touche, Ir a and Lasuye, T. and Xuereb, Catherine ( 2008) *[Jet injection studies for partially baffled mixing reactors: a general correlation for the jet trajectory and jet penetration depth.](#)* Chemical Engineering Research and Design, Vol.86 (n 10). pp. 1117-1127. ISSN 0263-8762

Any correspondence concerning this service should be sent to the repository administrator: [staff-oatao@inp-toulouse.fr](mailto:staff-oatao@inp-toulouse.fr)

# Jet injection studies for partially baffled mixing reactors: A general correlation for the jet trajectory and jet penetration depth

Jean-Philippe Torré<sup>a,b,c</sup>, David F. Fletcher<sup>b,\*</sup>, Irea Touche<sup>a</sup>,  
Thierry Lasuye<sup>c</sup>, Catherine Xuereb<sup>a</sup>

<sup>a</sup> Université de Toulouse, Laboratoire de Génie Chimique, CNRS/INP/UPS, Toulouse, France

<sup>b</sup> School of Chemical and Biomolecular Engineering, The University of Sydney, Sydney, NSW 2006, Australia

<sup>c</sup> LVM Quality and Innovation Department, Usine de Mazingarbe, Chemin des Soldats, 62160 Bully Les Mines, France

## A B S T R A C T

This paper is devoted to the analysis of the jet trajectories, obtained using computational fluid dynamics (CFD), at two different scales (laboratory and industrial) with application to quenching of runaway reactions. One of the goals was to describe how the jet penetrates the fluid in the stirred vessel and to build an easy to use correlation for research and industrial purposes. A model of the jet trajectory based on the analogy with a jet in a cross-flow has been used to predict the jet trajectory at the pilot and industrial scales. The correlation, built using a statistical analysis, has shown that the jet in a cross-flow model performs very well to describe the jet trajectories. A very interesting conclusion is that the correlation constants were found to be independent of scale. Finally, the authors proposed a definition of the penetration depth and use it in its dimensionless form to predict how the jet penetrates in the industrial vessel with the current injection conditions.

**Keywords:** Mixing; Runaway reaction; Jet penetration; Jet trajectory; Correlation; CFD

## 1. Introduction

The quenching of runaway reactions in industrial synthesis reactors is a very complex problem. Amongst the different inhibition systems and the possible alternatives reviewed by McIntosh and Nolan (2001), a jet injected at the surface of a stirred vessel is often used to quench an uncontrolled reaction for many reaction mixtures. McIntosh and Nolan (2001) highlighted that one of the main reasons that this system is not popular for industrial applications, despite its efficacy, is the lack of published information concerning the injection system, together with uncertainties over the mixing efficiency and distribution of the inhibitor within the bulk. The same conclusion was previously made by Rowe et al. (1994) and again more recently by Snee and Cusco (2005) and Bhattacharya and Kresta (2006). The problem of the quenching of runaway reactions by free-surface jet injections was investi-

gated recently by Torré et al., 2007a,b,c and Torré et al., 2008 for a partially baffled, agitated pilot reactor designed to represent an industrial model found in the polymer industry. Although the injection of reactants at the surface of stirred vessels is common in the chemical industry and has been previously studied by many authors (see for example Baldyga et al. (1993), Baldyga and Pohorecki (1995) and Verschuren et al. (2000)), no results were found in the literature concerning the trajectories of a fluid jet injected at the free-surface of an agitated vessel under batch operation conditions. In the present study, the authors have analysed numerical data for the jet trajectory, obtained using the commercial computational fluid dynamics (CFD) package ANSYS-CFX 11.0, for both pilot-scale and industrial reactors. The statistical analysis of these data, based on a simple jet in cross-flow analogy, allowed a general correlation to be proposed which describes, in good agreement with experimental data, the jet trajectory in the partially baffled

mixing vessel used in this study. Finally, the authors propose a definition of the jet penetration depth.

## 2. Model formulation

This work reported in this paper builds on previous modelling work in which a CFD model of fluid injection into a stirred vessel was developed. Details of the model can be found in [Torre et al. \(2008\)](#). Essentially, the modelling approach was to use a 3D CFD model to solve for the quasi-steady flow field in the mixing vessel in the absence of injection and then to inject transiently a fluid jet at the surface. The fluid in the jet was tracked using a scalar concentration. The jet trajectory was also predicted numerically using Lagrangian particle tracking of small “particles” that followed the flow. As the injection is transient, only the trajectory during the injection time was considered and the Lagrangian particles were not followed after the end of the injection time, as it is the initial trajectory of the jet that is of interest here. The jet trajectory and its behaviour have been described in detail in a previous paper ([Torre et al., 2008](#)) for the case of the pilot-scale partially baffled mixing reactor shown in [Fig. 1](#). The geometrical details of the pilot reactor and the injection system are listed in [Table 1](#).

Due to the 3D and transient nature of the flow (of both the jet and the agitated fluid) significant assumptions have to be made if a simplified model of the jet trajectory is to be developed. A 3D study of the jet trajectory would require a 3D function which could correlate the 3D plots represented by the Lagrangian particle tracks located in the whole vessel. Whilst this might be possible, the very different 3D jet behaviours observed and the complexity of the resulting trajectories would not yield a simple outcome to enable rapid prediction of injection behaviour, a key objective of this paper. Therefore, the correlation fitting was limited to two dimensions because this appeared to be the best way to describe the jet trajectories and is a first step to quantifying the jet penetration. The details of the system studied and the description of the coordinate system used are presented in [Figs. 1 and 2](#). [Fig. 1](#) gives details of the mixing vessel geometry and [Fig. 2](#) presents details of the jet location and the behaviour of the trajectory.

The jet trajectories considered for the correlation analysis correspond to the projection of the Lagrangian particle tracks onto a vertical plane, named the injection plane, and are defined by the point  $X_0, Y_0, Z_0$  and the unit vector pointing in the  $z$  direction which is normal to this plane. This process transforms the 3D data into two dimensions, and retains a good description of what is observed laterally, as shown in [Fig. 2\(b\)](#). As shown in [Fig. 2\(c\)](#), the jet is first deflected towards the vessel shell, and then it passes through the injection plane before spiralling in the central part of the vessel. Only the tracks having  $Z > Z_0$  have been considered to model the jet trajectory and all the data with  $Z < Z_0$  were discarded. This avoids confusion of the picture by the complicated behaviour of the trajectories in the vessel centre.

## 3. Analogy with jet in a cross-flow studies

The theoretical analysis which appeared to be the closest to the case studied here is that for liquid jets injected into a cross-flow ([Fig. 3](#)). As mentioned in [Muppidi and Mahesh \(2005\)](#), the dependency of the mean jet trajectory on the jet diameter is well-known and the flow field of a jet in a cross-flow

is believed to be influenced primarily by the effective velocity ratio  $R$  (which in this case simplifies to  $R = u_j/u_{cf}$ , where  $u_j$  is the jet velocity and  $u_{cf}$  is the cross-flow velocity). The reader can find further details on the subject in [Margason \(1993\)](#).

It was assumed that the equation which describes the jet trajectory in the case studied here is similar in form to that found in the literature for jets in cross-flows. This is clearly a significant assumption, as the velocity in the agitated vessel is not constant as usually considered for  $u_{cf}$  in jet in a cross-flow studies. The form of the equation which was chosen to model the jet trajectory in the agitated vessel was inspired by the correlations of [Ivanov \(1952, see Abramovich, 1963\)](#), [Shandorov \(1957, see Abramovich, 1963\)](#), [Gordier \(1963\)](#) and [Patrick \(1967\)](#). These very simple equations have proved to perform well in describing the trajectory of a jet injected normally into a cross-flow ([Rajaratnam, 1976](#)). These jet trajectory correlations are summarized in [Table 2](#).

To find an equivalent of the cross-flow velocity for the current problem, it was decided to consider the agitator tip-speed ( $U_{tip}$ ). It would be potentially interesting to consider a more accurate value of the bulk velocity which really impacts the fluid jet when it enters the vessel (for example, the integral of the tangential component of the bulk velocity on the vertical line normal to the injection surface in the upper part of the vessel). However such a measure is impractical if a simple correlation is to be established that is easy to apply. The agitator tip-speed, which gives the maximum velocity value in the vessel, gives an acceptable, scalable and practical parameter to use in the model.

The equations proposed in [Table 2](#) use a jet injection orifice centred at  $(X, Y) = (0, 0)$ . The cross-flow velocity and the jet velocity are directed toward  $O_x$  and  $O_y$ , respectively, as shown in [Fig. 3](#). For our case, the jet injection in the stirred vessel is located at the coordinates  $(X_0, Y_0$  and  $Z_0)$  where the origin of the coordinate frame is located at the bottom of the agitator (centre of the bottom dish).

A coordinate transformation is made using the following equation for the  $X, Y$  and  $Z$  coordinates, respectively:

$$\begin{cases} X^* = X - X_0 \\ Y^* = Y_0 - Y \\ Z^* = Z - Z_0 \end{cases} \quad (1)$$

The numerical values of  $X_0, Y_0$  and  $Z_0$ , expressed in metres, are  $(X_0, Y_0, Z_0) = (-0.094, 0.7, 0.1294)$  and  $(X_0, Y_0, Z_0) = (-0.66, 4.89, 0.90)$  for the pilot and industrial reactors, respectively. In agreement with the correlations listed in [Table 2](#), the jet trajectory is modelled using the form expressed in the following equation:

$$\frac{Y^*}{d} = A_1 \left( \frac{V}{U_{tip}} \right)^{A_2} \left( \frac{X^*}{d} \right)^B \quad (2)$$

## 4. Model fitting procedure

For each case analysed, the data for the Lagrangian particle tracks have been exported from the CFD simulation for times starting at zero to the final injection time. The data set has then been transformed using [Eq. \(1\)](#). Finally, only the data corresponding to  $Z^* > 0$  and  $X^* > 0$  have been conserved for further statistical analysis. These calculations were done using the commercial software Statgraphics Centurion XV both for the

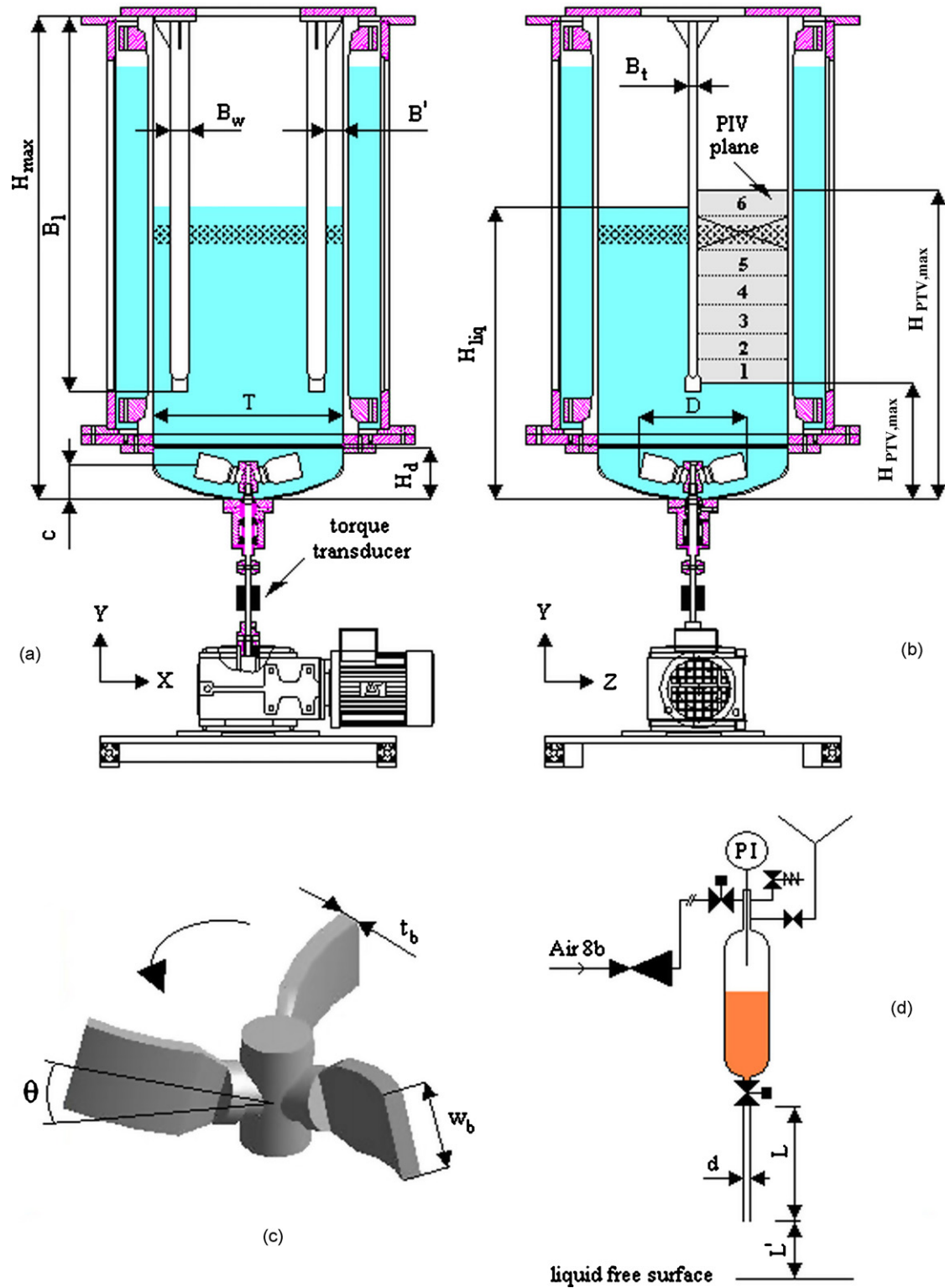


Fig. 1 – Details of the mixing vessel used in this study: (a) front view, (b) side view, (c) impeller and (d) jet injection system.

partially baffled vessel modelled at the laboratory and industrial scales.

The first analysis of the Lagrangian track data was performed by doing a non-linear fit of the cloud of points data from the CFD simulation to the following equation, using the Levenberg–Marquardt algorithm:

$$\frac{Y^*}{d} = A \left( \frac{X^*}{d} \right)^B \quad (3)$$

The Levenberg–Marquardt algorithm (or LMA), first published by Levenberg (1944) and rediscovered by Marquardt (1963), provides a numerical solution to the problem of minimizing a general non-linear function. The LMA interpolates between the Gauss–Newton algorithm (GNA) and the method of gradient descent. The LMA is more robust than the GNA, which means that in many cases it finds a solution even if it starts very far from the final minimum.

**Table 1 – Definition of the important dimensions and geometrical parameters of the experimental rig**

|  | Symbol               | Value      |
|--|----------------------|------------|
| Tank diameter (mm)                     | $T$                  | 450        |
| Maximum tank height (mm)               | $H_{\max}$           | 1156       |
| Bottom dish height (mm)                | $H_d$                | 122.9      |
| Agitator diameter (mm)                 | $D$                  | 260        |
| Number of agitator blades              | $n_b$                | 3          |
| Agitator blade width (mm)              | $w_b$                | 58         |
| Agitator blade thickness (mm)          | $t_b$                | 9          |
| Agitator retreat angle                 | $\theta$             | $15^\circ$ |
| Agitator clearance (mm)                | $c$                  | 47.2       |
| Baffles length (mm)                    | $B_l$                | 900        |
| Number of baffles                      | $n_B$                | 2          |
| Baffle width (mm)                      | $B_w$                | 46         |
| Baffle thickness (mm)                  | $B_t$                | 27         |
| Distance baffle-shell (mm)             | $B'$                 | 38.5       |
| Initial liquid height (mm)             | $H_{\text{liq}}$     | 700        |
| Injected volume (ml)                   | $V_i$                | 533        |
| Injection pipe diameter (mm)           | $d$                  | 10         |
| Injection pipe length (mm)             | $L$                  | 300        |
| Distance pipe outlet—free-surface (mm) | $L'$                 | 220        |
| Bottom height of the PIV plane (mm)    | $H_{\text{PIV,min}}$ | 278        |
| Top height of the PIV plane (mm)       | $H_{\text{PIV,max}}$ | 738        |

#### 4.1. Pilot-scale data

Thirteen simulations have been carried out for the pilot reactor. Nine of them were run with different jet diameter and the jet injection velocities but with the same agitator speed and four additional runs were devoted to the analysis of the influence of the agitator speed for a constant jet diameter and jet velocity. Fig. 4 shows the results of the non-linear fit to the Lagrangian particle track data for cases with varying jet diameters and injection speeds. A similar fit was obtained for the data at various agitator rotation rates (see [Torré \(2007\)](#) for details). The parameters obtained from the non-linear fitting which corresponds to these cases are given in Table 3.

#### 4.2. Industrial-scale data

Simulations have also been carried out for the industrial-scale reactor at two different agitator rotation speeds: the nominal speed ( $N_{\text{nom}}$ ) and half of the nominal speed ( $N_{\text{nom}}/2$ ).

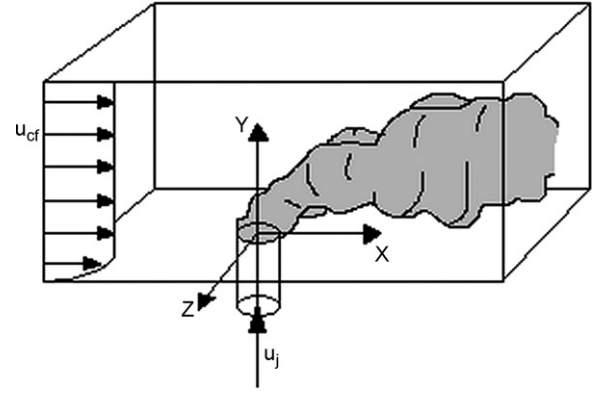


**Fig. 3 – Schematic of a jet in a cross-flow.**

The nominal speed and the jet velocity  $V_0$  are set to the real values used in the industrial polymerisation reactors. Four simulations have been carried out for each agitator speed, considering the jet diameter to remain constant at 100 mm and for jet velocities equal to  $V_0$ ,  $5V_0$ ,  $10V_0$ , and  $20V_0$ . Fig. 5 shows the results of the non-linear fit to the Lagrangian particle tracks and the results of the non-linear fit are given in Table 4.

#### 4.3. Determination of the model constants

The form of the law used to correlate the data gives good agreement between the model and the Lagrangian particle tracks in almost all cases. It may be noted that the constant  $B$  is of the same order of magnitude when considering either the pilot-scale or the industrial-scale with two exceptions for Fig. 5(a) and (e). These deviations are explained by the difficulty of fitting the model to the data from these two cases. Due to the low jet injection velocity, the “particles” accumulate very close to the free-surface and the jet shape is not well defined. The one-factor statistical analysis presented in the following paragraph give more details about this.

The 21 estimates for the constant  $B$  (pilot and industrial) have been analysed statistically and the results are represented in Fig. 6 using box-and-whiskers plots. The box-and-whisker plot, invented by [Tukey \(1977\)](#), is constructed by drawing: (i) a box extending from the lower quartile to the upper quartile. The middle 50% of the data values are

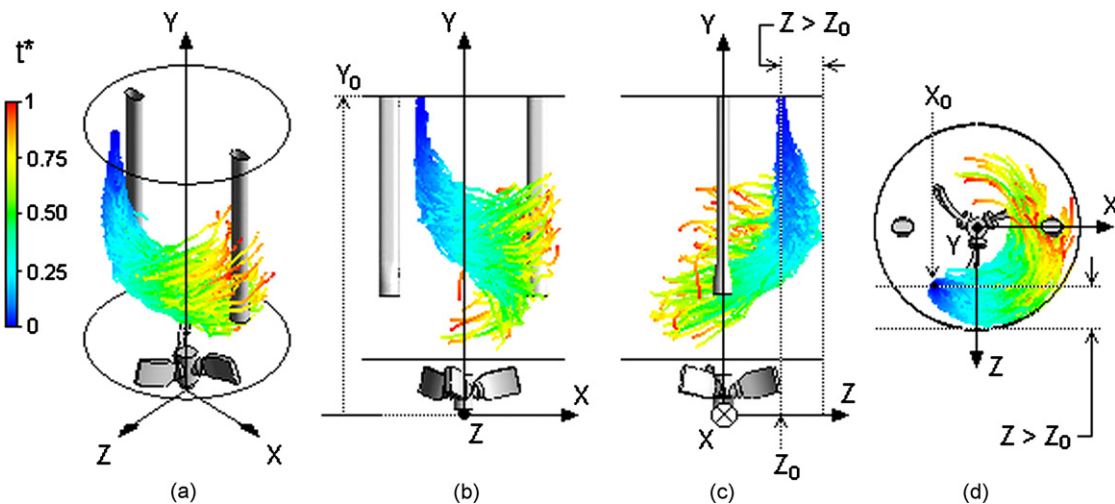


**Fig. 2 – Details of the coordinate system employed: (a) 3D view, (b) XY lateral view, (c) YZ lateral view and (d) XZ top view. The Lagrangian tracks are coloured by the particle travelling time normalized by the injection time (denoted as  $t^*$ ).**



**Table 2 – Correlations describing the penetration behaviour for circular jets injected normally into a cross-flow with  $R = u_j/u_{cf}$  (Rajaratnam, 1976)**

| Investigators                          | Equations  | Remarks   |
|--|--|---|
| Ivanov (1952, see Abramovich, 1963)    | $Y/d = R^{0.87}(X/d)^{0.33}$   | R was varied from 3.5 to about 32 and Ivanov also experimented with oblique jets<br>R was varied from 1.4 to 4.7 and Shandorov also experimented with oblique jets<br>Gordier worked with water jets in a water tunnel–axis joins maximum total pressure points<br>R varies from 6 to about 50. |
| Shandorov (1957, see Abramovich, 1963) | $Y/d = R^{0.79}(X/d)^{0.39}$   |   |
| Gordier (1963)                         | $Y/d = 1.31 R^{0.74}(X/d)^{0.37}$  |   |
| Patrick (1967)                         | $Y/d = R^{0.85}(X/d)^n$ ; $n = 0.38$ (from velocity measurements),<br>$n = 0.34$ (from concentration measurements) |   |

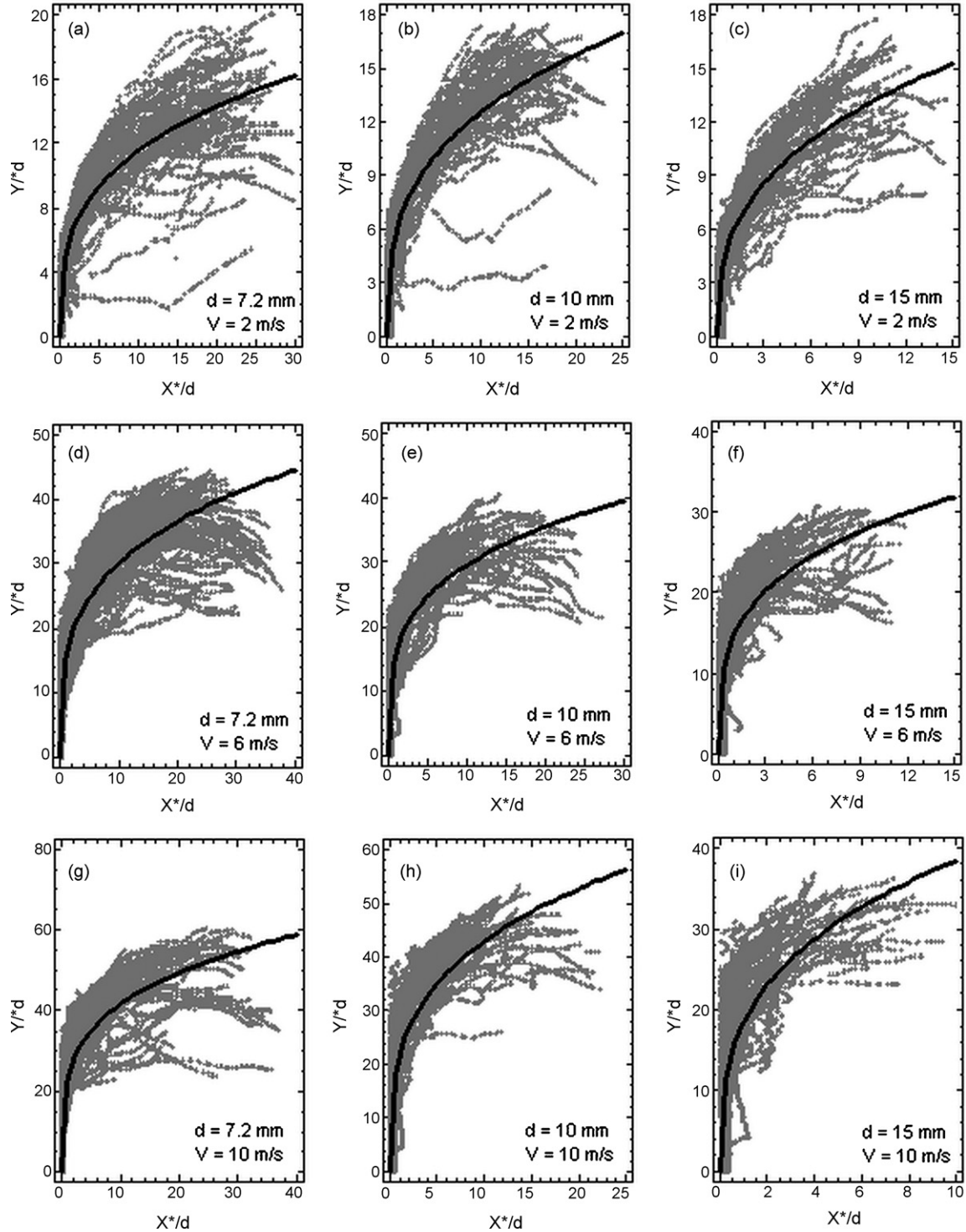


**Fig. 4 – Comparison between the Lagrangian particle tracks from CFD (grey symbols) and the jet trajectory correlation (black line) at  $N = 100$  rpm for the pilot reactor;  $N = 100$  rpm and  $U_{tip} = 1.36 \text{ m s}^{-1}$ .**

**Table 3 – Fitted A and B constants, 95% confidence interval (\*) and R-squared ( $R^2$ ) statistics (\*\*) (model  $(Y^*/d) = A(X^*/d)^B$  for the pilot reactor).**

|                  | A     | 95% confidence interval A (lower) | 95% confidence interval A (upper) | B    | 95% confidence interval B (lower) | 95% confidence interval B (upper) | $R^2$ (%) |
|------------------|-------|-----------------------------------|-----------------------------------|------|-----------------------------------|-----------------------------------|-----------|
| <b>Fig. 4</b>    |       |                                   |                                   |      |                                   |                                   |           |
| (a)              | 5.69  | 5.64                              | 5.75                              | 0.31 | 0.30                              | 0.31                              | 79.09     |
| (b)              | 5.93  | 5.89                              | 5.98                              | 0.33 | 0.32                              | 0.33                              | 81.97     |
| (c)              | 5.80  | 5.76                              | 5.85                              | 0.36 | 0.35                              | 0.36                              | 78.63     |
| (d)              | 15.68 | 15.62                             | 15.74                             | 0.28 | 0.28                              | 0.28                              | 80.41     |
| (e)              | 16.24 | 16.15                             | 16.32                             | 0.26 | 0.26                              | 0.26                              | 69.90     |
| (f)              | 14.87 | 14.78                             | 14.95                             | 0.28 | 0.28                              | 0.29                              | 57.72     |
| (g)              | 23.47 | 23.37                             | 23.57                             | 0.25 | 0.25                              | 0.25                              | 74.22     |
| (h)              | 21.93 | 21.81                             | 22.04                             | 0.29 | 0.29                              | 0.30                              | 67.92     |
| (i)              | 18.54 | 18.42                             | 18.65                             | 0.32 | 0.32                              | 0.32                              | 49.67     |
| <b>Not shown</b> |       |                                   |                                   |      |                                   |                                   |           |
| (a)              | 23.43 | 23.31                             | 23.55                             | 0.27 | 0.26                              | 0.27                              | 60.08     |
| (b)              | 19.77 | 19.69                             | 19.86                             | 0.27 | 0.26                              | 0.27                              | 72.49     |
| (c)              | 16.24 | 16.15                             | 16.32                             | 0.26 | 0.26                              | 0.26                              | 69.90     |
| (d)              | 14.25 | 14.19                             | 14.31                             | 0.28 | 0.27                              | 0.28                              | 77.18     |
| (e)              | 12.07 | 12.01                             | 12.12                             | 0.29 | 0.29                              | 0.29                              | 80.82     |

(\*) The confidence interval provides a bound when estimating a parameter for which the mean and standard deviation of the population can be estimated. From Fig. 4(a), we can conclude with 95% confidence that the A constant value is somewhere between 5.64 and 5.75. (\*\*)  $R^2$  is the percentage of the variability in  $Y^*/d$  that has been explained by the model. In this case, the non-linear regression against  $X^*/d$  explains about 79.09% of the variability in  $Y^*/d$ . The closer it is to 100%, the better the model has reproduced the data.

thus covered by the box; (ii) a vertical line at the location of the median, which divides the data in half; (iii) a cross sign at the location of the mean; (iv) whiskers extending from the quartiles to the largest and smallest observations, unless some values are far enough from the box to be

classified as “outside points”, in which case the whiskers extend to the most extreme points that are not classified as “outside”. “Outside” points are points more than 1.5 times the inter-quartile range above or below the limits of the box.

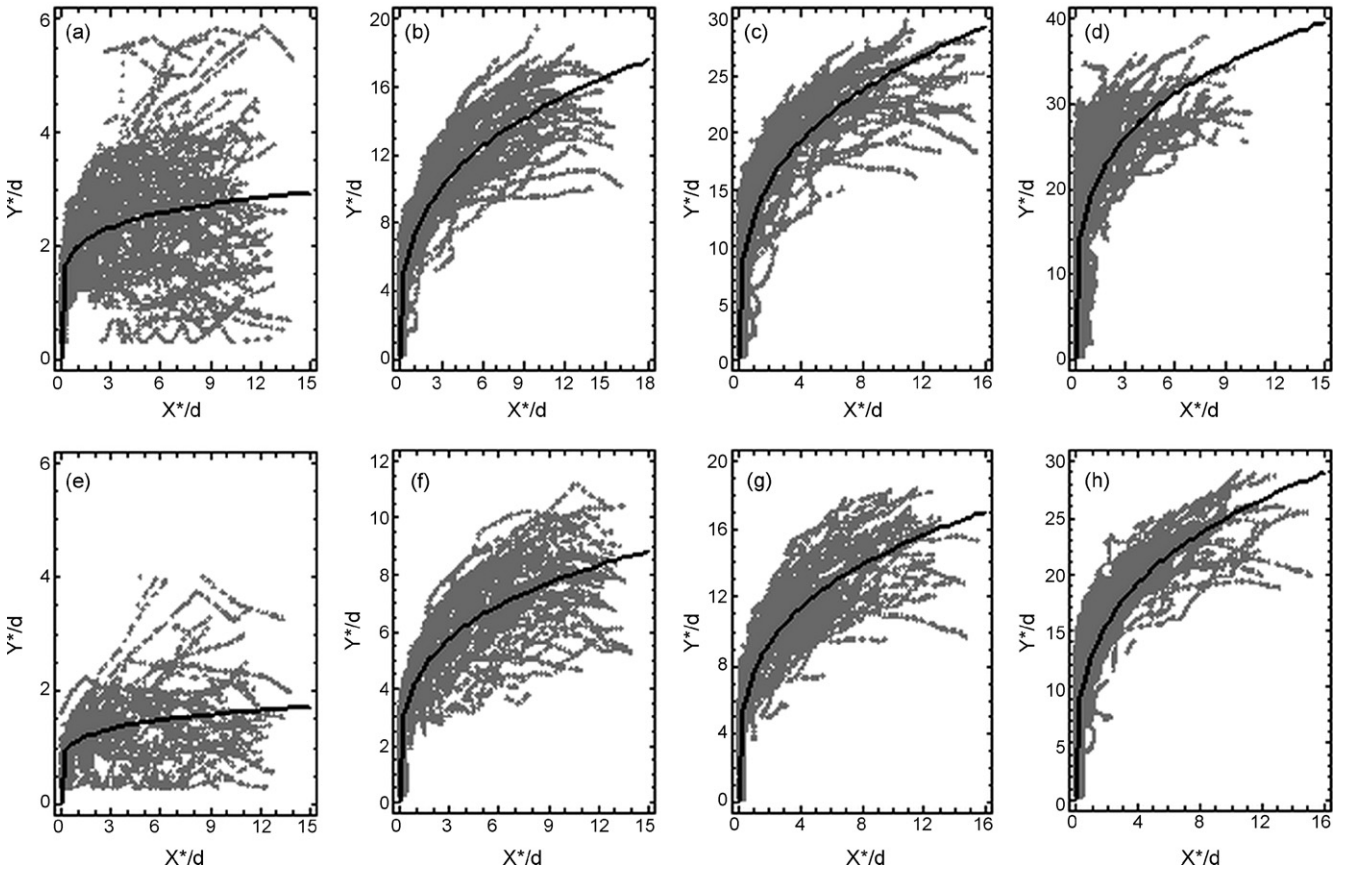


**Fig. 5 – Comparison between the Lagrangian particle tracks from CFD (grey symbols) and the jet trajectory correlation (black line) with  $d = 0.1$  m for the industrial reactor: (a)  $N_{nom}/2$ ,  $V = 1.55$  m  $s^{-1}$ ; (b)  $N_{nom}/2$ ,  $V = 7.75$  m  $s^{-1}$ ; (c)  $N_{nom}/2$ ,  $V = 15.5$  m  $s^{-1}$ ; (d)  $N_{nom}/2$ ,  $V = 31$  m  $s^{-1}$ ; (e)  $N_{nom}$ ,  $V = 1.55$  m  $s^{-1}$ ; (f)  $N_{nom}$ ,  $V = 7.75$  m  $s^{-1}$ ; (g)  $N_{nom}$ ,  $V = 15.5$  m  $s^{-1}$ ; (h)  $N_{nom}$ ,  $V = 31$  m  $s^{-1}$ .  $U_{tip} = 3.86$  and  $7.73$  m  $s^{-1}$  for  $N = N_{nom}/2$  and  $N_{nom}$ , respectively.**



**Table 4 – Fitted A and B constants, 95% confidence interval, and R-squared ( $R^2$ ) statistics (model  $(Y^*/d) = A(X^*/d)^B$  for the industrial reactor)**

| Fig. 5 | A     | 95% confidence interval A (lower) | 95% confidence interval A (upper) | B    | 95% confidence interval B (lower) | 95% confidence interval B (upper) | $R^2$ (%) |
|--------|-------|-----------------------------------|-----------------------------------|------|-----------------------------------|-----------------------------------|-----------|
| (a)    | 1.98  | 1.95                              | 2.01                              | 0.14 | 0.14                              | 0.15                              | 15.54     |
| (b)    | 7.12  | 7.08                              | 7.16                              | 0.31 | 0.31                              | 0.32                              | 81.14     |
| (c)    | 12.49 | 12.43                             | 12.54                             | 0.31 | 0.30                              | 0.31                              | 75.05     |
| (d)    | 19.55 | 19.45                             | 19.65                             | 0.26 | 0.26                              | 0.26                              | 56.40     |
| (e)    | 1.13  | 1.10                              | 1.16                              | 0.15 | 0.14                              | 0.17                              | 13.14     |
| (f)    | 4.29  | 4.26                              | 4.33                              | 0.27 | 0.26                              | 0.27                              | 73.22     |
| (g)    | 7.58  | 7.53                              | 7.62                              | 0.29 | 0.29                              | 0.29                              | 81.09     |
| (h)    | 12.69 | 12.62                             | 12.76                             | 0.30 | 0.29                              | 0.30                              | 74.46     |

As shown in Fig. 6(a), the values of B around 0.15, which correspond to Fig. 5(a) and (e), are outside the box. A substantial difference between the median and the mean indicates either the presence of an outlier or a skewed distribution. In the case of a skewed distribution, the mean would be pulled in the direction of the longer tail, which is not the case here. Thus, this confirms the two extreme points around 0.15 are outliers and must be deleted from the data set used to calculate the average value of the constant B. These deviations are explained by the bad non-linear fitting because the jet trajectory obtained with  $V = 1.55 \text{ m s}^{-1}$  gave clouds of points very close to the free-surface and the optimization method does not work well for large numbers of points without a well-defined form. Fig. 6(b) presents the analysis of the modified data set and the analysis of the 19 observations gave a mean value and standard deviation for B of 0.29 and 0.03, respectively. The standardized asymmetry and flatness values of 1.23 and 0.44 lie between  $-2$  and  $+2$ , indicating that the data set follows a normal distribution.

All the non-linear fits were re-calculated after setting the constant B to 0.29. In the model proposed for the correlation, the constant A depends on the quantity  $(V/U_{\text{tip}})$  with the form expressed in Eq. (4). The curve of  $\ln(A)$  versus  $\ln(V/U_{\text{tip}})$  used to estimate values for the  $A_1$  and  $A_2$  constants of Eq. (4) is shown in Fig. 7.

$$A = A_1 \left( \frac{V}{U_{\text{tip}}} \right)^{A_2} \quad (4)$$

The data are fitted extremely well by a straight line which means that a single correlation fits the data for the two reactors and that the proposed model constants are independent of the scale factor. Using the fitted data we

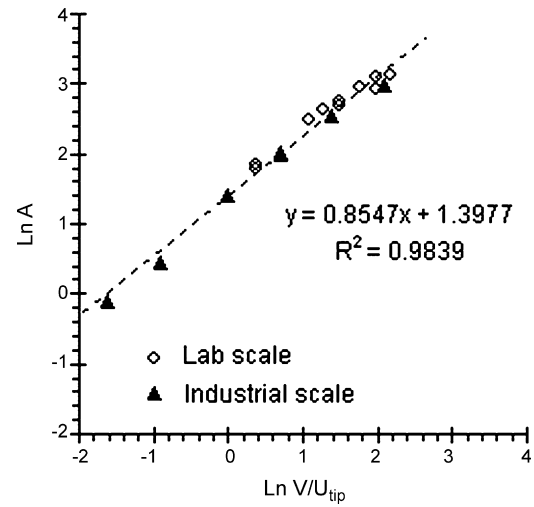


**Fig. 7 – A plot of  $\ln(A)$  versus  $\ln(V/U_{\text{tip}})$  for the pilot and the industrial reactor.**

obtain:

$$A = 4.05 \left( \frac{V}{U_{\text{tip}}} \right)^{0.85} \quad (5)$$

#### 4.4. Final correlation for the jet trajectory

The correlation is expressed in the following equation by

$$\frac{Y^*}{d} = 4.05 \left( \frac{V}{U_{\text{tip}}} \right)^{0.85} \left( \frac{X^*}{d} \right)^{0.29} \quad (6)$$

with  $0.072 \text{ m} \leq d \leq 0.1 \text{ m}$ ,  $0.68 \text{ m s}^{-1} \leq U_{\text{tip}} \leq 7.73 \text{ m s}^{-1}$  and  $0 \leq X^* \leq -2X_0$  ( $X_0 < 0$ ).

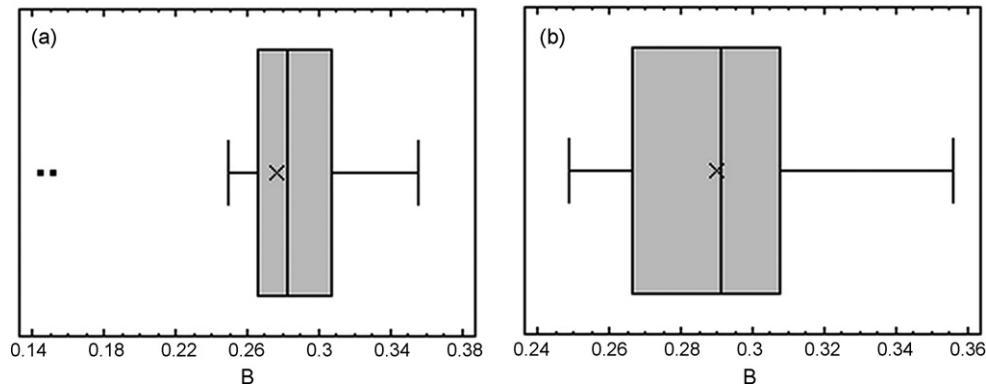


**Fig. 6 – Box and whiskers plots of B: (a) complete data set; (b) data set without outliers.**

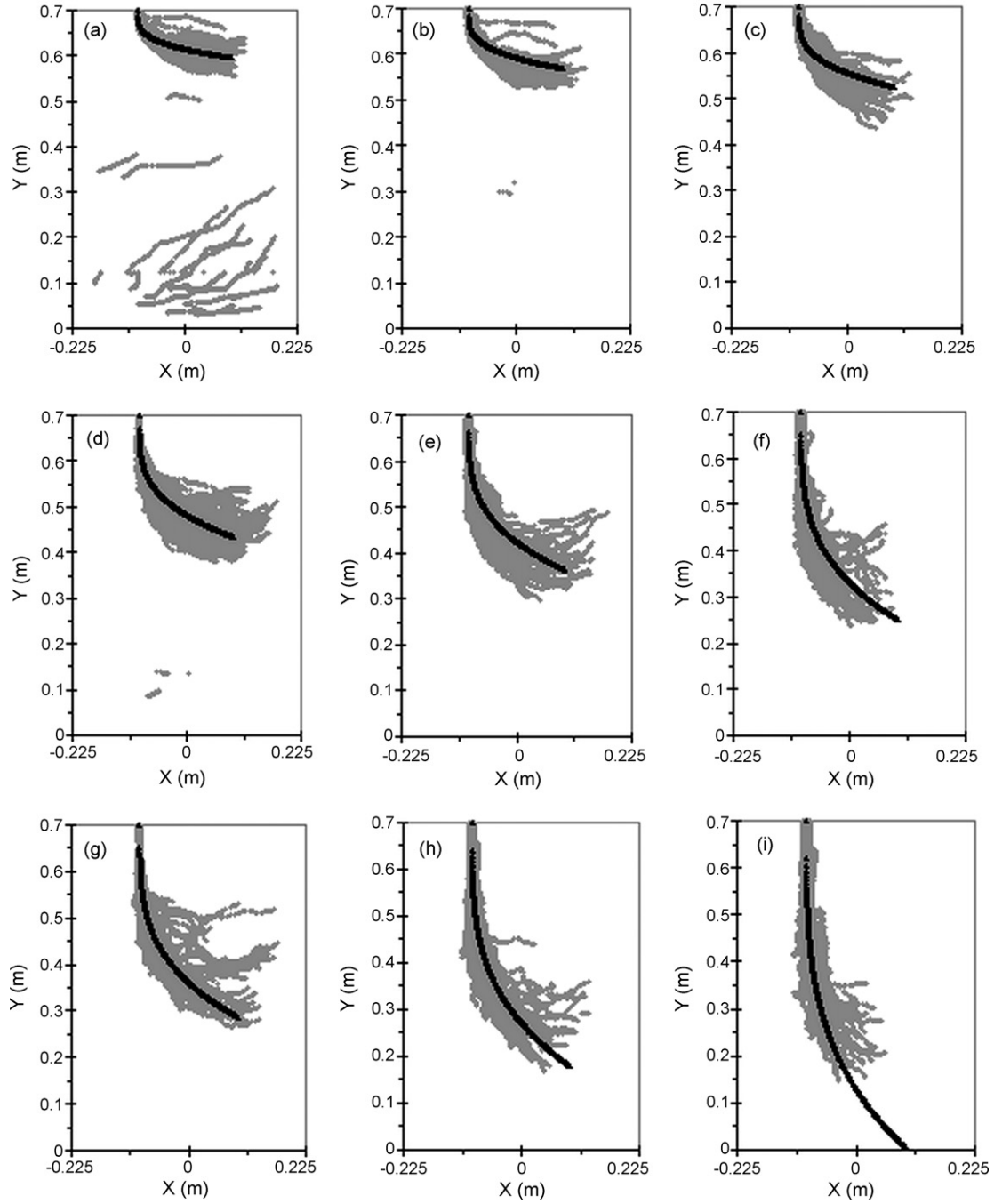


**Fig. 8 – Comparison between the Lagrangian particle tracks from CFD (grey symbols) and the jet trajectory obtained by using Eq. (7) (black line) at  $N = 100$  rpm for the pilot reactor: (a)  $d = 7.2$  mm,  $V = 2$  m s<sup>-1</sup>; (b)  $d = 10$  mm,  $V = 2$  m s<sup>-1</sup>; (c)  $d = 15$  mm,  $V = 2$  m s<sup>-1</sup>; (d)  $d = 7.2$  mm,  $V = 6$  m s<sup>-1</sup>; (e)  $d = 10$  mm,  $V = 6$  m s<sup>-1</sup>; (f)  $d = 15$  mm,  $V = 6$  m s<sup>-1</sup>; (g)  $d = 7.2$  mm,  $V = 10$  m s<sup>-1</sup>; (h)  $d = 10$  mm,  $V = 10$  m s<sup>-1</sup>; (i)  $d = 15$  mm,  $V = 10$  m s<sup>-1</sup>.**

An important result is that the correlation is independent of the reactor scale and the jet trajectory  $Y = f(X)$  is expressed in the following equation as

$$Y = Y_0 - d \left[ 4.05 \left( \frac{V}{U_{\text{tip}}} \right)^{0.85} \left( \frac{X - X_0}{d} \right)^{0.29} \right] \quad (7)$$

and is valid for  $0.072 \text{ m} \leq d \leq 0.1 \text{ m}$  and  $0.68 \text{ m s}^{-1} \leq U_{\text{tip}} \leq 7.73 \text{ m s}^{-1}$  and  $X_0 \leq X \leq -X_0$  ( $X_0 < 0$ ).

Eq. (7) is compared with the Lagrangian particle tracks in physical coordinates for the pilot and industrial reactors in Figs. 8-10. It is clear that the proposed model is able to describe the CFD data for the jet trajectory with very good agreement

for various jet injection and agitation conditions. One of the most important results is that the correlation is found to be the same for the laboratory and the industrial scales. Surprisingly, the constants  $A_1$  and  $A_2$  found here for a completely different situation to that of a jet in a cross-flow are very similar in value to those presented in Table 2.

## 5. Comparison with experimental data

Torré et al. (2008) presented a technique to average experimental data to remove stochastic variations. Essentially, jet injection was performed three times for nominal identical conditions to allow an estimation of the random variabil-

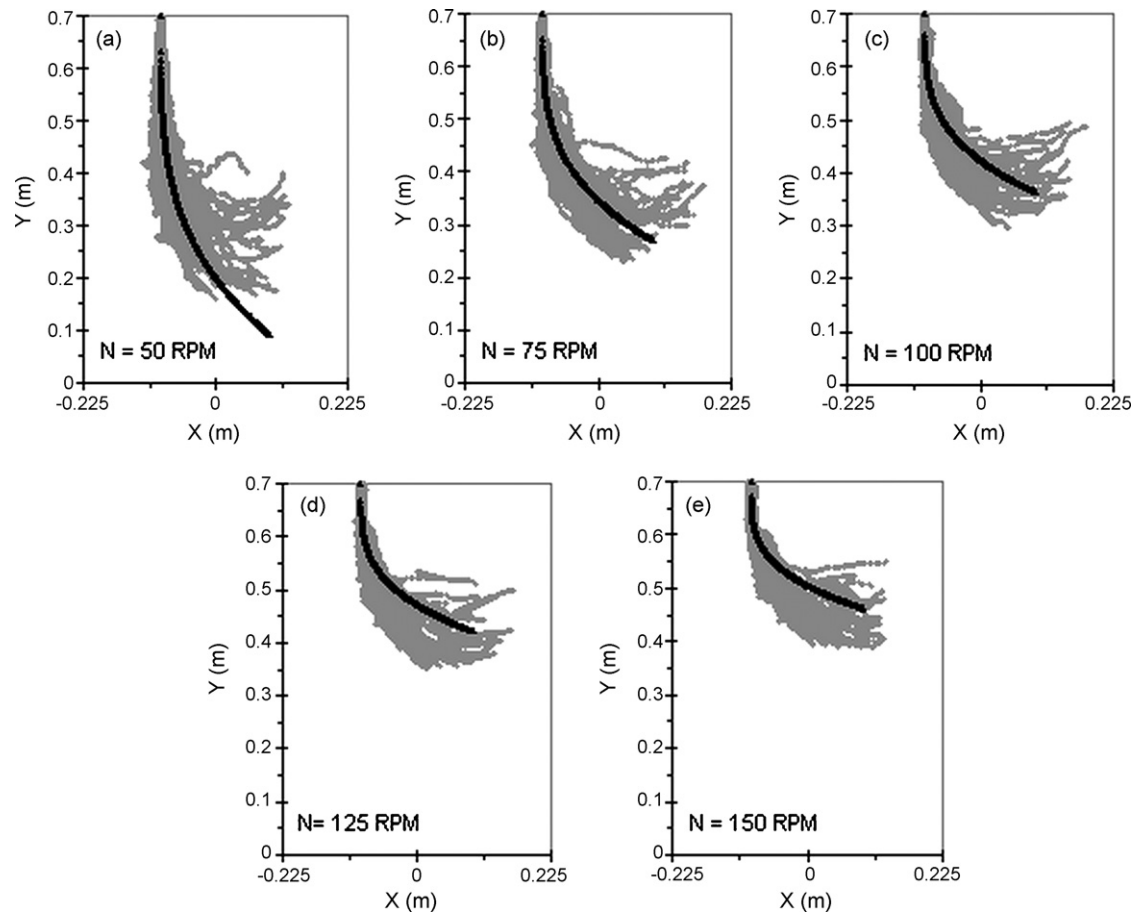


Fig. 9 – Comparison between the Lagrangian particle tracks from CFD (grey symbols) and the jet trajectory obtained by using Eq. (7) (black line) with  $d = 10 \text{ mm}$  and  $V = 6 \text{ m s}^{-1}$  for different agitator rotation speeds (pilot reactor).

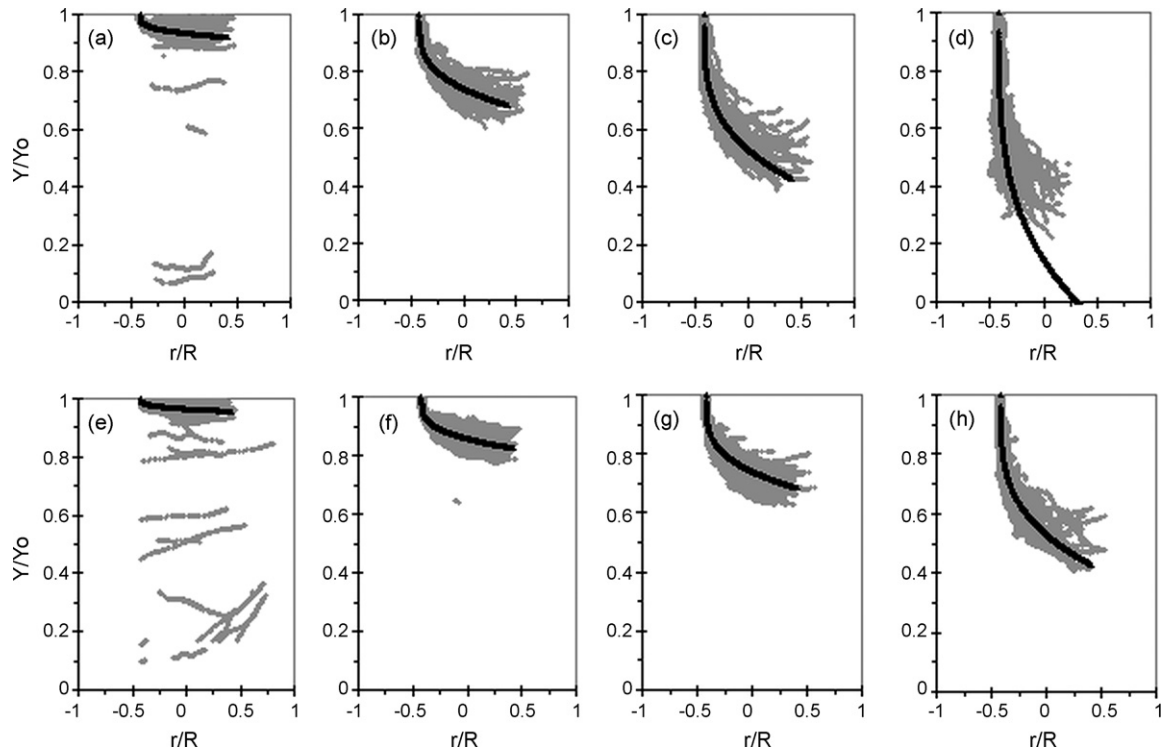
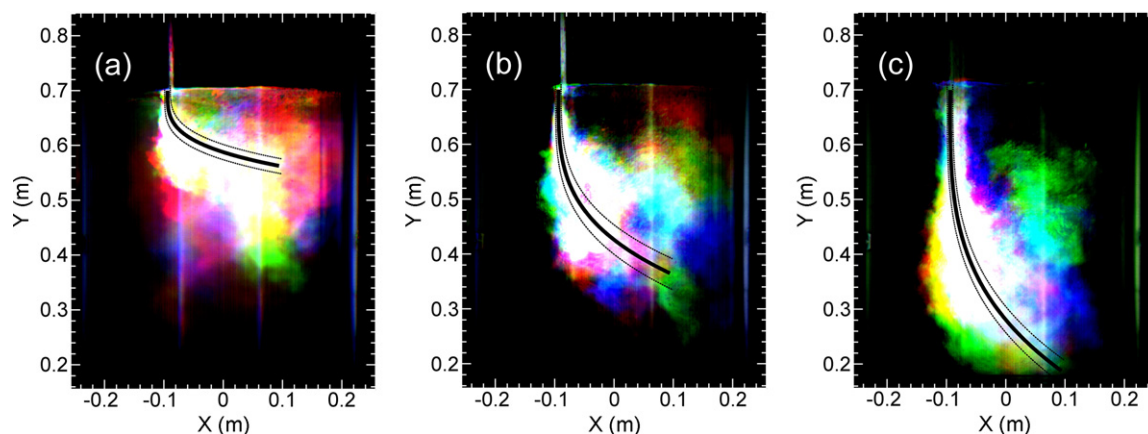


Fig. 10 – Comparison between the Lagrangian particle tracks from CFD (grey symbols) and the jet trajectory obtained by using Eq. (7) normalized (black line) with  $d = 0.1 \text{ m}$  for the industrial reactor: (a)  $N_{\text{nom}}/2$ ,  $V = 1.55 \text{ m s}^{-1}$ ; (b)  $N_{\text{nom}}/2$ ,  $V = 7.75 \text{ m s}^{-1}$ ; (c)  $N_{\text{nom}}/2$ ,  $V = 15.5 \text{ m s}^{-1}$ ; (d)  $N_{\text{nom}}/2$ ,  $V = 31 \text{ m s}^{-1}$ ; (e)  $N_{\text{nom}}$ ,  $V = 1.55 \text{ m s}^{-1}$ ; (f)  $N_{\text{nom}}$ ,  $V = 7.75 \text{ m s}^{-1}$ ; (g)  $N_{\text{nom}}$ ,  $V = 15.5 \text{ m s}^{-1}$ ; (h)  $N_{\text{nom}}$ ,  $V = 31 \text{ m s}^{-1}$ .



**Fig. 11 – Comparison between experimental pictures of jet injections obtained using the trichromy imaging process and the theoretical jet trajectory correlation (full line) at  $N = 100$  rpm. (a)  $V = 2.1 \pm 0.1 \text{ m s}^{-1}$ ; (b)  $V = 6.0 \pm 0.5 \text{ m s}^{-1}$ ; (c)  $V = 9.9 \pm 0.6 \text{ m s}^{-1}$ . The dotted lines show the uncertainty limits for each trajectory predicted by the correlation.**

ity of the process and the jet penetration was recorded via the trichromy imaging process described previously in Torr  (2007) and in Torr  et al. (2008). In short, a fluorescent tracer (Fluorescein) is incorporated into the injected liquid and all the experiments were done under UV light produced by two blacklight tubes (Philips TL-D, 120/26,  $\lambda_{\text{max}} = 355 \text{ nm}$ ). The jet penetration into the stirred liquid was recorded using a high speed black and white camera (HCC-1000 from VDS Vossk hler monitored by the NV1000 software from New Vision Technologies). At the end of the injection time, the three pictures obtained from the three different experiments for the jet trajectory on an XY plane were colour transformed; one into red, one into green and one into blue. Finally, these three elementary frames were superimposed. The area common to the three experiments appeared white, resulting from the additive synthesis of the RGB imaging technique.

Fig. 11 shows a comparison of the experimental data for three different jet velocities at  $N = 100$  rpm with the predictions obtained from the correlation. This demonstrates clearly that the correlation describes the jet trajectory in this vessel very well in both a qualitative and quantitative sense.

## 6. Conclusions

A correlation has been developed that can be used to predict the penetration behaviour of a jet into a mixing vessel and provides a useful technique for exploring the efficacy of jet injection systems used to quench runaway reactions. The correlation was developed using a computational fluid dynamics model to predict the behaviour of an injected jet into a partially baffled stirred vessel. The correlation is based on the form used for a jet in a cross-flow and uses the impeller tip-speed as a measure of the cross-flow velocity. The correlation is shown to fit well for a wide range of injection and agitation speeds for both pilot and industrial-scale systems. Direct comparison with experimental data confirms the validity of the approach.

## Acknowledgements

Tessengerlo Group and ANRT are acknowledged for financial support. The authors owe great thanks to the technical staff of the LGC of Toulouse. A part of the computer resources needed was provided by the Scientific Grouping CALMIP and the authors would like to acknowledge N. Renon for enabling this

to happen. Special thanks are given to Damien Mateo for his assistance with the image post-treatment of the jet pictures.

## References

- Abramovich, G.N., 1963, The theory of turbulent jets (English translation published by M.I.T. Press, Massachusetts).
- Baldyga, J., Bourne, J.R. and Yang, Y., 1993, Influence of feed pipe diameter on mesomixing in stirred tank reactors. *Chem. Eng. Sci.*, 48(19): 3383–3390.
- Baldyga, J. and Pohorecki, R., 1995, Turbulent micromixing in chemical reactors—a review. *Chem. Eng. J. Biochem. Eng. J.*, 58(2): 183–195.
- Bhattacharya, S. and Kresta, S.M., 2006, Reactor performance with high velocity surface feed. *Chem. Eng. Sci.*, 61(9): 3033–3043.
- Gordier, R.L., 1963, Studies on fluid jets discharging normally into moving liquid (St. Anthony Falls Hydraulics Laboratory, University of Minnesota, MN), Tech. Paper, 28, Ser. B.
- Levenberg, K., 1944, A method for the solution of certain non-linear problems in least squares. *Quart. Appl. Math.*, 2(2): 164–168.
- Margason, R.J., 1993, Fifty years of jet in cross flow research, *Proc. AGARD, Computational and Experimental Assessment of Jets in Cross Flow*, 1.1–1.41.
- Marquardt, D., 1963, An Algorithm for least-squares estimation of nonlinear parameters. *SIAM J. Appl. Math.*, 11: 431–441.
- McIntosh, R.D. and Nolan, P.F., 2001, Review of the selection and design of mitigation systems for runaway chemical reactions. *J. Loss Prevent. Process Ind.*, 14(1): 27–42.
- Muppidi, S. and Mahesh, K., 2005, Study of trajectories of jets in crossflow using direct numerical simulations. *J. Fluid Mech.*, 530: 81–100.
- Patrick, M.A., 1967, Experimental investigation of the mixing and penetration of a round turbulent jet injected perpendicularly into a transverse stream. *Trans. Inst. Chem. Eng.*, 45, T, 16–31.
- Rajaratnam, N., (1976). *Developments in Water Science: Turbulent Jets*. (Elsevier Scientific Publishing Co, New York, USA).
- Rowe, S.M., Nolan, P.F. and Starkie, A.J., 1994, The control of runaway polymerisation reactions by inhibition techniques. *ICHEME Symp. Ser.*, 134: 575–587.
- Snee, T.J. and Cusco, L., 2005, Pilot-scale evaluation of the inhibition of exothermic runaway. *Trans IChemE, Part B, Process Safe. Environ. Protect.*, 83(B2): 135–144.
- Torr , J.P., 2007, Quenching runaway reactions: hydrodynamics and jet injection studies for agitated reactors with a deformed free-surface, Ph.D. Thesis, Universit  de Toulouse and University of Sydney.
- Torr , J.P., Fletcher, D.F., Lasuye, T. and Xuereb, C., 2007, An experimental and computational study of the vortex shape in a partially baffled agitated vessel. *Chem. Eng. Sci.*, 62(7): 1915–1926.

- Torré, J.P., Fletcher, D.F., Lasuye, T. and Xuereb, C., 2007, Transient hydrodynamics and free surface capture of an under-baffled stirred tank during stopping. *Chem. Eng. Res. Des.*, 85(A5): 626–636.
- Torré, J.P., Fletcher, D.F., Lasuye, T. and Xuereb, C., 2007, Single and multiphase CFD approaches for modelling partially baffled vessels: comparison of experimental data with numerical predictions. *Chem. Eng. Sci.*, 62(22): 6246–6262.
- Torré, J.P., Fletcher, D.F., Lasuye, T. and Xuereb, C., 2008, An experimental and CFD study of liquid jet injection into a partially-baffled mixing vessel: a contribution to process safety by improving the quenching of runaway reactions. *Chem. Eng. Sci.*, 63(4): 924–942.
- Tukey, J.W., 1977, *Exploratory Data Analysis*, EDA, Reading, MA (Addison-Wesley).
- Verschuren, I., Wijers, J. and Keurentjes, J., 2000, Mixing with a Pfaudler type impeller: the effect of micromixing on reaction selectivity in the production of fine chemicals, In *Proceedings of the 10th European Conference on Mixing*, pp. 69–75.